C. R. Acad. Sci. Paris, Sciences de la Terre et des planètes / Earth and Planetary Sciences 333 (2001) 591–599

S1251-8050(01)01677-9/FLA

Tectonique / Tectonics

Stress transfer and seismicity changes before large earthquakes

David D. Bowman, Geoffrey C.P. King*

Laboratoire de tectonique et mécanique de la lithosphère, Institut de physique du Globe de Paris, 4, place Jussieu, 75252 Paris cedex 05, France

Received 26 March 2001; accepted 25 September 2001

Abstract – In recent years, observational and theoretical descriptions of spatio-temporal patterns of seismicity have focused on two fundamental (and controversial) observations: static stress (Coulomb) interactions between earthquakes and accelerating seismic moment release before large earthquakes. While there have been several documented examples of static stress changes influencing the space-time pattern of seismicity *following* great earthquakes (main shocks and aftershocks), there have been few attempts to link this method to the evolution of seismicity *before* great earthquakes (precursory seismicity and foreshocks). In this paper, we describe a simple physical model that links static stress modeling to accelerating moment release before a large event. For practical reasons, it is not straightforward to apply this technique as a method of forecasting future large earthquakes. However, after the large event has occurred, the region of stress accumulation can be calculated with precision based on the known source parameters of the earthquake. This region can then be examined for seismic moment rate changes prior to the event. As examples, we have examined all $M \geqslant 6.5$ earthquakes in California since 1950 in regions defined by their pre-event stress fields, and find a period of accelerating moment release before all of these events. While we illustrate the model using seismicity in California, the technique is general and can be applied to any tectonically active region. Where sufficient knowledge of the regional tectonics exists, this method can be used to augment current techniques for seismic hazard estimation. © 2001 Académie des sciences / Éditions scientifiques et médicales Elsevier SAS

earthquake / California / stress transfer / accelerating seismicity / Coulomb stress

Résumé – Les transferts de contraintes et les changements de sismicité avant les grands séismes. Ces dernières années, les descriptions empiriques et théoriques des changements spatio-temporels dans la sismicité se sont concentrées sur deux observations fondamentales : les interactions de la contrainte statique de Coulomb entre les séismes et l'accélération de l'activité sismique avant un fort tremblement de terre. Alors qu'il y a eu de nombreux exemples de variation de la contrainte statique influençant la distribution spatio-temporelle de la sismicité, il n'y a eu que peu de tentatives pour relier cette méthode à l'évolution de la sismicité *avant* de grands tremblements de terre (précurseurs sismiques). Dans ce papier, nous décrivons un modèle physique simple qui lie les modèles de contrainte statique à l'accélération de l'activité sismique avant un fort tremblement de terre. Pour des raisons pratiques, il n'est pas facile de transformer cette technique en une méthode de prédiction de futurs grands tremblements de terre. Cependant, après l'arrivée d'un fort séisme, la région où les contraintes se sont accumulées peut être caractérisée avec précision, puisque les paramètres du séisme sont bien connus. Cette région peut ensuite être examinée pour rechercher

* Correspondence and reprints.
E-mail address: king@ipgp.jussieu.fr (G.C.P. King).

une accélération potentielle de l'activité sismique. Nous avons ainsi examiné tous les séismes de magnitude $M \geqslant 6{,}5$ en Californie depuis 1950 et les régions alentour définies par les champs de contraintes avant ces séismes, et trouvé une période d'accélération de la sismicité avant tous ces événements. Même si nous illustrons ce modèle en utilisant la sismicité de la Californie, cette technique est générale et peut être appliquée à toute région tectoniquement active. Dans les régions où la connaissance de la tectonique est suffisante, cette méthode peut être utilisée pour obtenir une meilleure estimation du risque sismique.

séismes / Californie / contrainte transférée / accélération de l'activité sismique / contrainte de Coulomb

1. Background

1.1. Accelerating Moment Release

It has long been suggested that large earthquakes are preceded by observable variations in regional seismicity. Some of the earliest work on this subject was conducted by Kiyoo Mogi, who demonstrated an observable increase in the level of seismicity in surrounding regions before great shallow earthquakes in Japan (the so-called 'Mogi Doughnut') [23–25]. It was in this context that Mogi [24] and Fedotov [11] formulated the idea of a seismic cycle. Following these pioneering works, many authors have documented increased seismicity prior to large earthquakes. Ellsworth, Lindh, Prescott and Herd [10] reported an increase in the rate of earthquakes $M \geqslant 5$ in the years prior to the 1906 San Francisco earthquake in a broad region covering much of the San Francisco Bay area. Lindh [20] documented similar increases in intermediate magnitude seismicity before the 1707 $M \approx 8.3$ Kwanto, 1857 $M \approx 8.1$ Fort Tejon, and 1923 $M = 8.2$ Tokyo earthquakes.

In recent years there has been a growing effort to describe these observed periods of enhanced seismicity using a variety of analytic functions [4–7, 15, 30, 38, 41]. Numerous mechanisms have been proposed to explain these observations, including heterogeneous bond-breaking models (e.g. [32]), hierarchical fiber-bundle models (e.g. [27]) and classical damage mechanics (e.g. [21]). Some workers have suggested that damage mechanics on a regional scale may lead to a runaway process of faulting that would be observed as an increased rate of seismicity prior to large earthquakes. Bufe and Varnes [6] pointed out that a simple power-law time-to-failure equation derived from damage mechanics could be used to model the observed seismicity. They demonstrated that the seismicity before the 1989 $M = 7.0$ Loma Prieta earthquake was well fit by a relation of the form (equation (1)):

$$\varepsilon(t) = A + B\,(t_c - t)^m \tag{1}$$

where t_c is the time of the large event, B is negative and m is usually about 0.3. A is the value of $\varepsilon(t)$ when $t = t_c$, i.e., the final Benioff strain up to and including the largest event. The cumulative Benioff strain at time t is defined as (equation (2)):

$$\varepsilon(t) = \sum_{i=1}^{N(t)} E_i(t)^{1/2} \tag{2}$$

where E_i is the energy of the ith event and $N(t)$ is the number of events at time t.

In contrast to the above are models where the crust is in a state of 'intermittent criticality' (e.g. [3, 13, 34]). This hypothesis is an outgrowth of efforts to characterise large earthquakes as a critical phenomenon [1, 2, 8, 17, 31, 33, 38, 39], and suggests that a large earthquake is the end result of a process in which the stress field becomes correlated over increasingly long scale-lengths. The scale over which the stress field is correlated sets the size of the largest earthquake that can be expected at that time. The largest event possible in a given fault network cannot occur until regional criticality has been achieved. This large event then destroys criticality on its associated network, creating a period of relative quiescence after which the process repeats by rebuilding correlation lengths towards criticality and the next large event.

Sornette and Sammis [38] and Sammis et al. [35] pointed out that the power-law time to failure relation in equation (1) is also to be expected if the seismic cycle is modeled as a critical phenomenon. Bowman et al. [4] tested the predictions of this hypothesis by searching for 'critical regions' before recent large earthquakes in California. They found that before all earthquakes $M \geqslant 6.5$ from 1950 to 1998 along the San Andreas system in California, there was a well-defined period of accelerating seismic energy release within a finite region that scaled with the size of the impending large earthquake. They further defined a 'curvature parameter' that quantified the quality of the power-law fit to the observed seismicity and aided in the determination of the critical region. Based on the number of events and the quality of the curve fits it was shown that the null hypothesis that purely random clustering could generate the observed acceleration in seismicity could be rejected at greater than 95 % confidence. Furthermore, they observed that the radius of the critical region found using this

method scales with the magnitude of the associated large event. Subsequent studies by other workers (e.g. [5, 15, 28]) have reproduced these results in the New Madrid Seismic Zone, New Zealand, and the Aegean.

1.2. Coulomb stress changes and earthquake interactions

The observations and models described above are strongly tied to concepts of statistical physics. As such, they pay little or no attention to the actual mechanism of stress transfer between events. However, many studies have demonstrated that the static stress changes from previous earthquakes have a strong influence on the location, and presumably the timing, of subsequent seismicity. Such works include the observation of stress shadows following great earthquakes (e.g. [12, 15, 37]) and Coulomb stress triggering of seismicity (e.g. [19, 26, 40]). Common to these studies is the observation that seismicity can be strongly influenced by small changes in the static stress field. An important implication of this is that prior to an earthquake, stress must accumulate not only on the fault itself but also in a large region surrounding the fault. Consequently, defining this region has become a major objective of Coulomb stress interaction studies.

The precise definition of regions of increased static stress requires modeling the contributions of events over a long period of time. Instrumental seismic data, GPS data, InSAR data and field observations of surface rupture all combine to make calculation of the stress fields of recent earthquakes routine. However, the source parameters of pre-instrumental earthquakes are significantly more difficult to define. For such calculations, it is necessary to combine the historical and geological record of seismicity with the long-term loading to define regions that have been stressed by prior earthquakes [9, 14, 22, 40]. As shown by recent models of the Marmara region following the Izmit earthquake [14, 29], different interpretations of historical data can significantly alter the interpretation of the modeled stress field. The difficulty of this technique is further highlighted by the fact that the tectonic and historical information available for the Sea of Marmara region is perhaps the most detailed information in the world. A stark contrast is the difficulty in accounting for the recent $M = 7.1$ Hector Mine Earthquake. This event, which occurred in a region that many people considered to be in a 'stress shadow' of the 1992 $M = 7.3$ Landers event, was well within the coverage of one of the densest and most advanced seismic and geodetic networks in the world. However, little is known of the long-term tectonic and seismic evolution of the region, which may explain the difficulty that Coulomb models have accounting for the occurrence of this event. On this basis it might seem that defining regions of pre-earthquake stress with any accuracy will be difficult to achieve.

2. Negative earthquakes and the pre-earthquake stress field

As described above, most efforts to describe the stress field before large earthquakes have been based on models of the historical activity prior to the event. An idealized summary of this method is illustrated in *figure 1a*. Slip on faults near the surface predominantly act to relieve stresses, creating large stress shadows. Countering this effect is loading at depth through fault creep, which creates a broad region of increased stress around the future failure plane. However, if the large event has already occurred a simpler method is to calculate the stress field required to move a fault with the observed orientation, displacement, and rake of the large event.

This approach rests on the concept of elastic rebound, which is that the stress released in an earthquake existed as a pre-stress prior to the event (*figure 1b*). In general, the stress existing before rupture on a fault of finite length can be determined by calculating the stress that results from slipping the fault backwards by the amount that it moved in the earthquake [36], the so-called 'negative earthquake'. The resulting Coulomb stress field can then be calculated using well-established techniques (see [18]). This effectively produces the same field that would result from an accurate knowledge of the tectonic history and loading mechanism in the region (*figure 1a*). For dip-slip earthquakes, only the horizontal part of the slip is required to model the pre-stress since the stresses that load the system are predominantly horizontal and motion is not purely elastic rebound for these events (*figure 1c*).

3. Pre-earthquake stress and accelerating moment release

We now use the distribution of static (Coulomb) stress before an earthquake to determine the regions expected to show accelerating moment release before the event, using the methodology described above and in *figure 1b*. The Coulomb pre-stress field is calculated based on a simple slip model of the earthquake under consideration. The pre-event seismicity is then iteratively tested for accelerating activity within a range of calculated Coulomb stress values. At each stress value, the cumulative Benioff strain of earthquakes within the stress contour (*figure 1b*) is fitted to a power-law time-to-failure function and to a straight

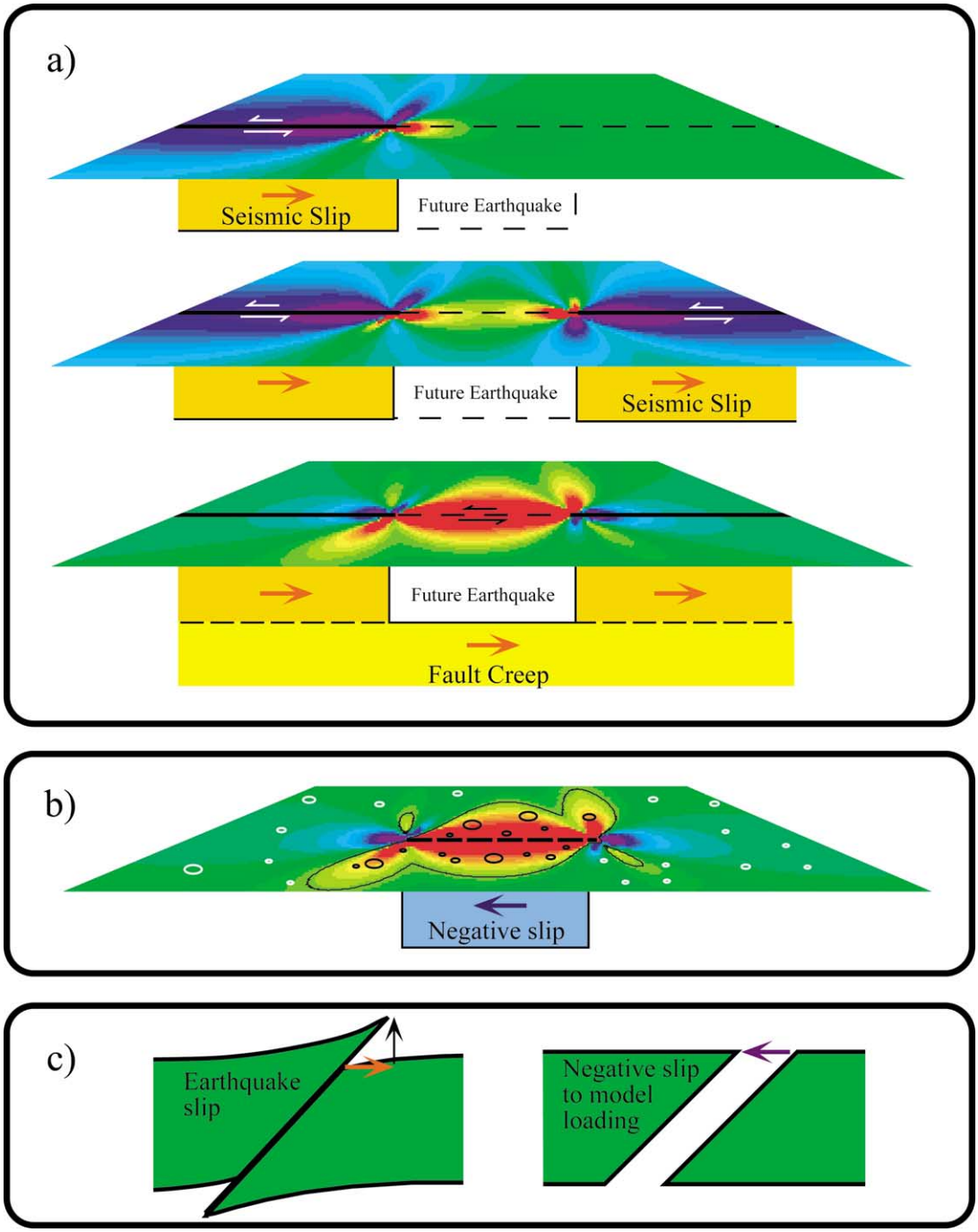

Figure 1. Evolution of Coulomb stresses prior to an earthquake. The Coulomb stress is calculated by the usual methods. Friction is assumed to be 0.4. A regional stress orientated at 45° to the fault favours strike-slip faulting in the same sense as the main event (or antithetic to it). **a.** The stress state prior to the earthquake is composed of two parts. Earthquakes occur along strike in both directions, plus loading by aseismic slip on the fault below seismogenic depths. **b.** For a strike-slip fault this stress can be modelled by reversing the sense of slip observed to occur in the earthquake. Other parameters are as in **a.** Regions where stress must have been high prior to the main event are examined for accelerated moment release. The choice of the contour bounding the region is discussed in the text. **c.** Dip-slip events are associated with permanent deformation and not simple elastic rebound. This is modelled by adopting the negative of the horizontal component of slip.

Figure 1. Évolution des contraintes de Coulomb avant un séisme. La contrainte de Coulomb est calculée par les méthodes habituelles. La friction est de 0,4. La contrainte régionale des failles, orientée à 45°, favorise un mouvement décrochant dans le même sens que le séisme principal (ou antithétique). **a.** L'état de contrainte avant un séisme se compose de deux parties. Des séismes ont lieu de part et d'autre du futur séisme ; une mise en charge par glissement asismique sur la faille en dessous de la région sismogénique a lieu. **b.** Pour une faille décrochante, cet état de contrainte peut être modélisé en inversant le sens du glissement qui a eu lieu durant le séisme. Les autres paramètres sont comme en **a.** On recherche si l'activité sismique a augmenté dans les régions où les contraintes étaient élevées avant le séisme principal. Le choix du contour exact de la région est discuté dans le texte. **c.** Les séismes en failles normales ou inverses sont associés à une déformation permanente ; il n'existe pas de modèle de rebond élastique simple. Ils sont modélisés ici en utilisant l'inverse de la composante horizontale du glissement.

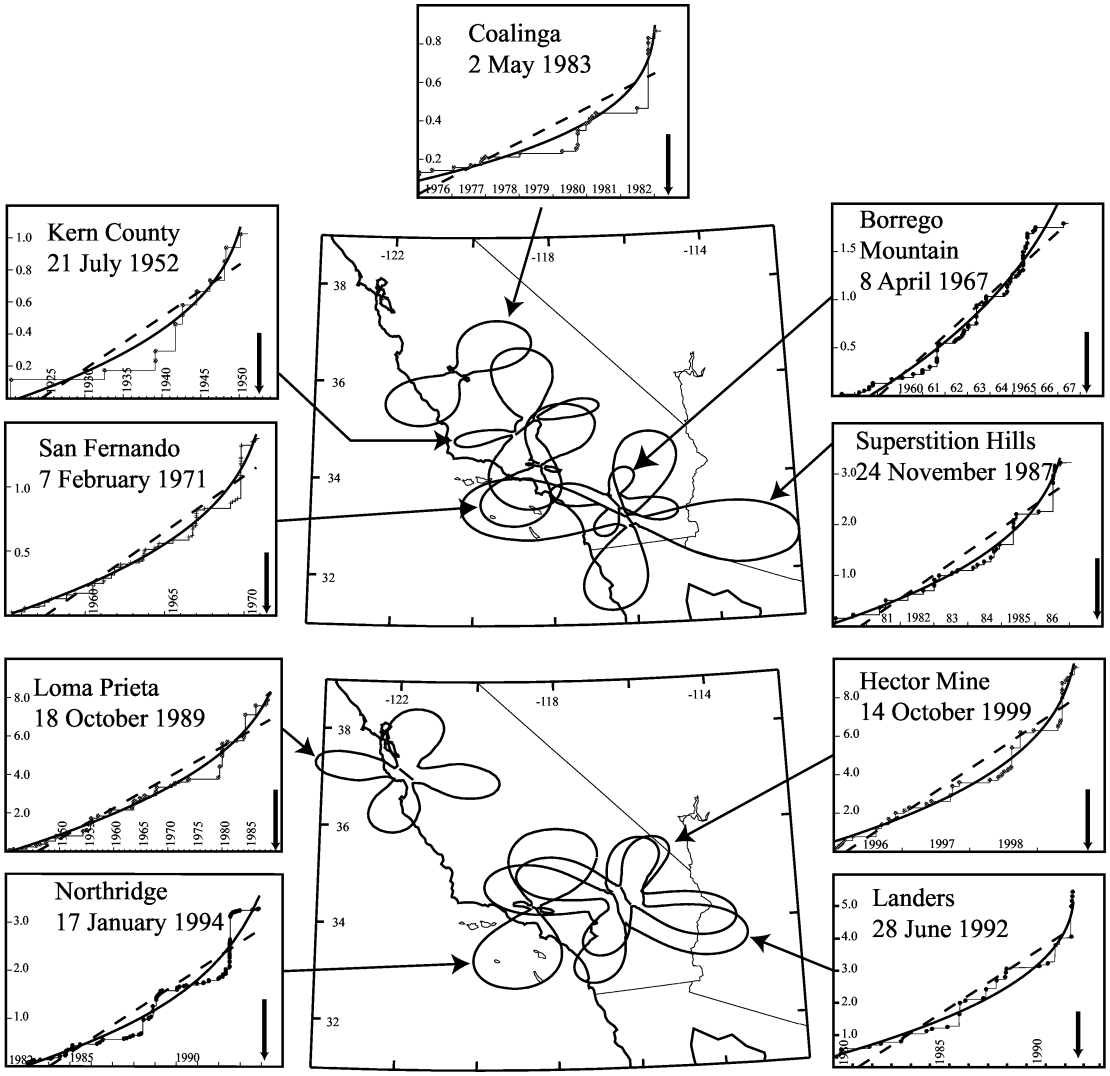

Figure 2. Critical regions and cumulative Benioff strain for all events $M \geqslant 6.5$ since 1950 in central and southern California. The solid curves in the cumulative Benioff strain plots are the fit of the data to the power-law time-to-failure equation, while the dashed lines are the fit of the data to a straight line (see text for details), with the time of the main event in each sequence indicated by a vertical arrow. The maps show the Coulomb stress contour used to define the critical region for each of the corresponding seismicity curves. The *table* lists the value of the stress contour and the parameters of the curve fit for each event.

Figure 2. Les régions critiques et les déformations cumulées de Benioff pour tous les séismes de magnitude $M \geqslant 6{,}5$ depuis 1950 dans le Sud et le Centre de la Californie. Les données sont approximées au mieux ou par des courbes – trait continu – représentant une loi de puissance temps–rupture ou par une droite – trait pointillé – (voir texte pour les détails) ; l'arrivée du séisme principal dans chacune des séquences temporelles est marquée d'une flèche.

line. We define a curvature parameter as the ratio of the residuals to the power-law fit to the residuals of the linear fit. Thus, accelerating sequences will have a curvature parameter less than 1, linear sequences will have a curvature parameter of 1, and decelerating sequences will be greater than 1. The critically stressed region is then defined as the Coulomb stress contour that minimizes the curvature parameter and is thus a meaningful determination of the critical region (see [4, 5]). The method for defining the critical region in this study is similar to the methodology established by Bowman et al. [4], with the important difference that the region is not defined by varying the size of an arbitrary volume, but rather by searching over the range of Coulomb stress values determined by the pre-stress of the impending earthquake.

We apply this method to all of the $M \geqslant 6.5$ earthquakes in central and southern California since 1950. Detailed source models are not necessary when calculating the far-field stress distributions required [18], thus uniform average slip distributions are adequate for all the Coulomb calculations. For each of the

Table. Summary of parameters used to model the accelerating moment release. Stress cut-off is the contour value defining the region where events are fitted to the power-law time-to-failure function. Minimum magnitude is the lowest magnitude in the catalog used in the curve fitting. The catalog is known to be complete at or below this magnitude in all cases except the Kern County event. The quality of the earthquake catalogs before 1952 is questionable.

Tableau. Rappel des paramètres utilisés pour modéliser l'accélération de l'activité sismique. Le seuil de contrainte est la valeur de contour de la région où les séismes sont ensuite approximés par une loi de puissance temps–rupture. La magnitude minimale est la plus petite magnitude du catalogue utilisée. On sait que le catalogue est complet au niveau ou en dessous de cette magnitude, sauf dans le cas du séisme de Kern County. La qualité du catalogue avant 1952 est problématique.

Event/*Séisme*	Date	Magnitude	Stress cutoff/ *Seuil de contrainte* (bar)	Minimum magnitude/ *Magnitude minimale*	T_f	Curvature parameter/ *Paramètre de courbure*
Kern County	21 July 1952	7.5	0.05	4.6	1952.2	0.56
Borrego Mountain	8 April 1968	6.5	0.1	3.5	1968.8	0.71
San Fernando	9 February 1971	6.6	0.01	3.5	1971.4	0.49
Coalinga	2 May 1983	6.7	0.01	3.5	1983.0	0.49
Superstition Hills	24 November 1987	6.6	0.01	3.5	1987.0	0.39
Loma Prieta	18 October 1989	7.0	0.1	4.5	1990.8	0.49
Landers	28 June 1992	7.3	0.1	4.5	1992.4	0.36
Northridge	17 January 1994	6.7	0.005	3.5	1995.7	0.58
Hector Mine	14 October 1999	7.1	0.1	3.5	1999.6	0.47

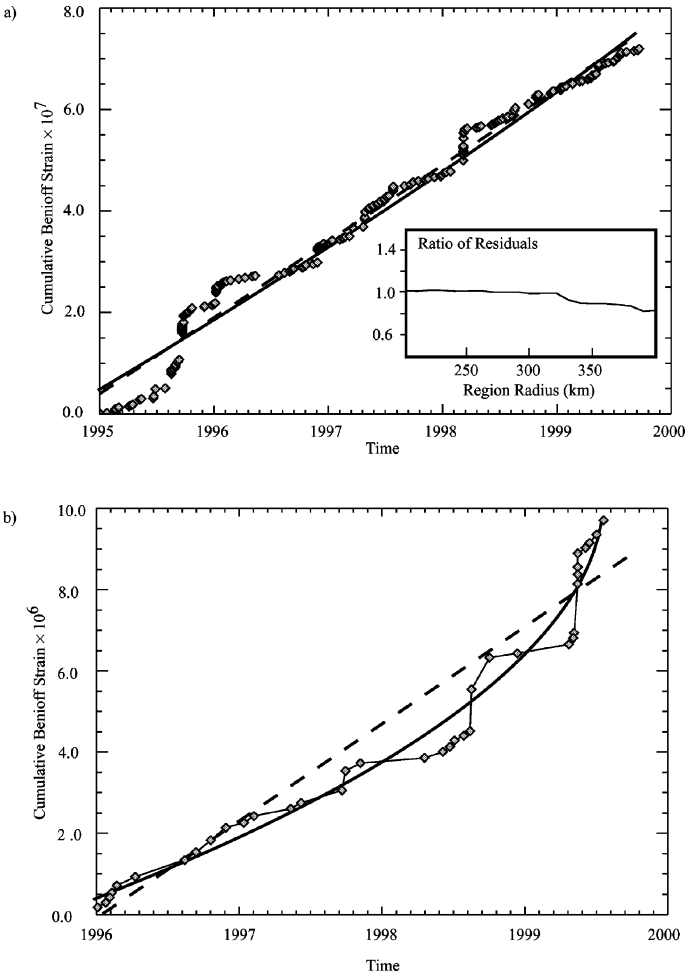

Figure 3. Cumulative Benioff strain release before the 1999 $M_w = 7.1$ Hector Mine earthquake. **a.** Cumulative Benioff strain release in a 300 km radius circular region. The scaling of earthquake magnitude with region radius found by Bowman et al. [4] and Jaumé and Sykes [6] suggests that this is the appropriate region size for an $M = 7.1$ event; however, there is no acceleration in the region. The inset shows the ratio of the linear and power-law curve fits, as defined by Bowman et al. [4]. The relatively constant ratio of residuals near to one indicates that, before the Hector Mine event, no accelerating moment release can be found for any region between 200 and 400 km radius. **b.** Cumulative Benioff strain release in a positive stress change contour of 0.1 bar. There is clear acceleration in the seismicity within this region.

Figure 3. Évolution des déformations cumulées de Benioff avant le séisme d'Hector Mine de magnitude $M_w \geqslant 7{,}1$ de 1999. **a.** Évolution des déformations cumulées de Benioff dans une région circulaire de 300 km de rayon. Ce dernier paramètre est obtenu en utilisant une relation d'échelle entre la magnitude du séisme et le rayon de la région à considérer, relation trouvée par Bowman et al. [4] et Jaumé et Sykes [6] ; il n'y a cependant pas d'accélération de la sismicité dans la région ainsi définie. L'encart montre la différence entre une approximation des données linéaires et par une loi de puissance, telle qu'elle a été définie par Bowman et al. [4]. Cette différence est quasiment nulle, ce qui indique qu'avant le séisme d'Hector Mine, aucune accélération de l'activité sismique n'a pu être trouvée, quelle que soit la région de 200 à 400 km de rayon considérée. **b.** Évolution des déformations cumulées de Benioff dans la région où les contraintes ont augmenté d'au moins 0,1 bar. On observe une claire augmentation de la sismicité dans cette région.

events in our study, a Coulomb stress field contour is found that defines the region of precursory accelerating activity (*figure 2*). The parameters of the region optimization (including the chosen contour) are listed in the *table*. Also listed is the asymptote of the power-law time-to-failure function (equation (1)). As pointed out by Bufe and Varnes [7] and Sornette and Sammis [38], the asymptote time, t_c, should correspond to

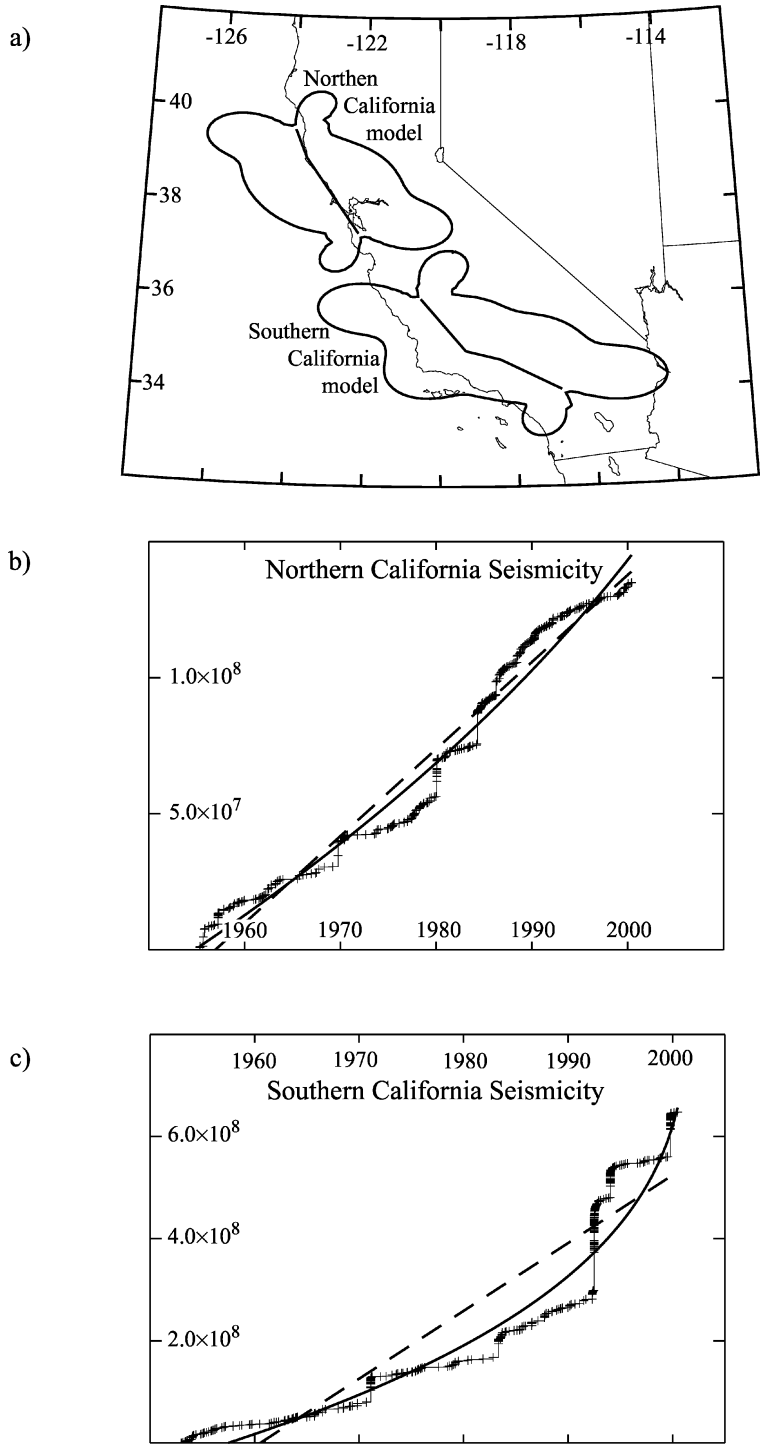

Figure 4. Stress contours and associated cumulative Benioff strain for model events in northern and southern California. **a.** Map showing static stress contours used to select seismicity. The northern California model shows the 0.2 bar stress change contour based on a rupture of the San Andreas Fault north of the segments that ruptured in the 1989 Loma Prieta earthquake. The southern California model shows the 0.2 bar stress change contour based on a rupture from Parkfield to San Gorgonio Pass. **b.** Cumulative Benioff strain for earthquakes in the 0.2 bar contour for the northern California model. There is no evidence for accelerating moment release in the observed seismicity. **c.** Cumulative Benioff strain in the 0.2 bar contour for the southern California model. Accelerating moment release is clear. The fit to a power-law time-to-failure equation (see methods) yields an asymptote time of 2001.68.

Figure 4. Les courbes de contrainte et les déformations cumulées de Benioff pour des séismes majeurs dans le Nord et le Sud de la Californie. **a.** Carte montrant les contours de la contrainte statique utilisés pour sélectionner la sismicité. Le modèle du Nord de la Californie montre la courbe d'augmentation de la contrainte de 0,2 bar liée à la rupture de la faille de San Andreas au nord des segments qui ont rompu lors du séisme de Loma Prieta en 1989. Le modèle du Sud de la Californie donne la courbe d'augmentation de la contrainte de 0,2 bar liée à une rupture entre Parkfield et San Gorgonio Pass. **b.** Évolution des déformations cumulées de Benioff pour les séismes se trouvant à l'intérieur de la courbe de 0,2 bar, dans le Nord de la Californie. Il n'y a pas d'accélération de la sismicité dans les données actuelles. **c.** Évolution des déformations cumulées de Benioff, à l'intérieur de la courbe de 0,2 bar, pour le Sud de la Californie. Une accélération de l'activité sismique est visible. En approximant les données par une loi de puissance temps/rupture, on obtient une rupture en 2001,68.

the time of the actual event. Examination of the *table* shows that this is the case.

It is worth remarking that the methodology described here is able to find a region of accelerating moment release before the 1999 $M = 7.1$ Hector Mine Earthquake. However, circular critical regions as described by Bowman et al. [4] are unable to find a corresponding period of accelerating moment release (*figure 3*) before the event. This further suggests that the method described here provides a more appropriate definition of the critical region before a large earthquake.

4. Discussion and conclusions

The examples that we offer suggest that the region of increased activity before a large earthquake can be

identified with the area that must have been subject to an increase of stress prior to the event; the larger the event, the larger the region. Previous work that has searched for circular critical regions has found that the radius of the region scales as the magnitude of the great earthquake being 'predicted' by the acceleration [4, 5, 16]. Unlike circular regions, areas of increased Coulomb stress loading provide a natural explanation for both the widely distributed increase of seismicity before large events and the observed scaling of the region size. Because the spatial extent of the stress perturbation caused by an earthquake scales with the moment of the event, or in this case the impending event, the mechanism described above provides a natural explanation for the observed scaling.

The method described in this paper is designed to examine precursory activity after the event has already occurred. However, two areas can be identified where existing geological knowledge gives an indication of the probability of a large earthquake in the coming decades; the San Andreas Fault near San Francisco and the Fort Tejon segment of the southern San Andreas. The Working Group on California Earthquake Probabilities (WGCEP) has assigned a very low probability (2 %) for another event on the segments of the San Andreas that ruptured in the 1906 San Francisco earthquake [42] and a high probability (18–28 %) of an event on the segments of the San Andreas fault that ruptured in the 1857 Ft. Tejon earthquake [43]. The pre-stress field for a repetition of either of these events can easily be calculated using the Negative Earthquake approach described above. Analyzing the seismicity in the two calculated regions results in similar conclusions (*figure 4*) to the WGCEP reports. For the northern San Andreas, no region can be found which displays accelerating moment release while accelerating moment release is clear in southern California.

Finally we emphasize that the use of this technique as method of earthquake prediction should be approached with caution, since the method requires forehand knowledge of the fault or fault segments that will rupture in a future event. As recent earthquakes such as Landers, Northridge, Kobe, Hector Mine, and Bhuj have illustrated, this frequently is not the case. Using our procedure, the region of increased stress is clearly easier to identify *after* the event than *before* it. Prediction is much harder when it concerns the future. Nevertheless, our approach has allowed us to elucidate an important feature of the underlying physics of the earthquake cycle that should be incorporated into models of regional seismicity and seismic hazard.

Acknowledgements. The authors acknowledge discussions with Charles Sammis and James Dolan. This work was supported by a Châteaubriand Post-Doctoral Fellowship sponsored by the French Embassy to the United States (DDB), EC Environment Programs (FAUST and PRESAP) and CNRS INSU Grant (contribution number 290). IPGP contribution number 1761.

References

[1] Allègre C.-J., Le Mouël J.-L., Introduction of scaling techniques in brittle failure of rocks, Phys. Earth Planet. Inter. 87 (1994) 85–93.

[2] Allègre C.-J., Le Mouël J.-L., Provost A., Scaling rules in rock fracture and possible implications for earthquake predictions, Nature 297 (1982) 47–49.

[3] Bowman D.D., Sammis C.G., Intermittent criticality and the seismic cycle, Bull Seismol. Soc. Am. (submitted).

[4] Bowman D.D., Ouillon G., Sammis C.G., Sornette A., Sornette D., An observational test of the critical earthquake concept, J. Geophys. Res. 103 (1998) 24359–24372.

[5] Brehm D.J., Braile L.W., Intermediate-term earthquake prediction using precursory events in the New Madrid seismic zone, Bull. Seismol. Soc. Am. 88 (1998) 564–580.

[6] Bufe C.G., Varnes D.J., Predictive modelling of the seismic cycle of the greater San Francisco bay region, J. Geophys. Res. 98 (1993) 9871–9883.

[7] Bufe C.G., Nishenko S.P., Varnes D.J., Seismicity trends and potential for large earthquakes in the Alaska-Aleutian region, Pageoph 142 (1994) 83–99.

[8] Chelidze T.L., Percolation and fracture, Phys. Earth Planet. Inter. 28 (1982) 93–101.

[9] Deng J., Sykes L.R., Evolution of the stress field in southern California and triggering of moderate-size earthquakes: a 200-year perspective, J. Geophys. Res. 102 (1997) 9859–9886.

[10] Ellsworth W.L., Lindh A.G., Prescott W.H., Herd D.J., The 1906 San Francisco Earthquake and the seismic cycle, in: Simpson D.W., Richards P.G. (Eds.), Earthquake Prediction: An International Review, Maurice Ewing Ser., Vol. 4, AGU, Washington, DC, 1981, pp. 126–140.

[11] Fedotov S.A., Regularities in the distribution of strong earthquakes in Kamchatka, the Kuriles, and northeastern Japan, Akad. Nauk USSR Inst. Fiz. Aml.: Trudy 36 (1965) 66–95.

[12] Harris R.A., Simpson R.W., In the shadow of 1857: the effect of the great Ft. Tejon earthquake on subsequent earthquakes in southern California, Geophys. Res. Lett. 23 (1996) 229–232.

[13] Huang Y., Saleur H., Sammis C.G., Sornette D., Precursors, aftershocks, criticality and self-organized criticality, Europhys. Lett. 41 (1998) 43–48.

[14] Hubert-Ferrari A., Barka A., Jacques E., Nalbant S.S., Meyer B., Armijo R., Tapponnier P., King G.C.P., Seismic hazard in the Marmara Sea following the 17 August 1999 Izmit earthquake, Nature 404 (2000) 269–273.

[15] Jaumé S.C., Sykes L.R., Evolution of moderate seismicity in the San Francisco Bay region, 1850 to 1993: Seismicity changes

related to the occurrence of large and great earthquakes, J. Geophys. Res. 101 (1996) 765–789.

[16] Jaumé S.C., Sykes L.R., Evolving towards a critical point: a review of accelerating moment/energy release prior to large and great earthquakes, Pure Appl. Geophys. 155 (1999) 279–306.

[17] Keilis-Borok V.I., The lithosphere of the Earth as a large nonlinear system, in: Garland G.D., Apel J.R. (Eds.), Quo Vadimus: Geophysics for the Next Generation, Geophys. Monogr. Ser., Vol. 60, AGU, Washington, DC, 1990, pp. 81–84.

[18] King G.C.P., Cocco M., Fault interaction by elastic stress changes: new clues from earthquake sequences, Adv. Geophys. 44 (2001) 1–38.

[19] King G.C.P., Stein R.S., Lin J., Static stress changes and the triggering of earthquakes, Bull. Seismol. Soc. Am. 84 (1994) 935–953.

[20] Lindh A.G., The seismic cycle pursued, Nature 348 (1990) 580–581.

[21] Lyakhovsky V., Ben-Zion Y., Agnon A., Earthquake cycle, fault zones and seismicity patterns in a rheologically layered lithosphere, J. Geophys. Res. (in press).

[22] Matsuura M., Jackson D.D., Cheng A., Dislocation model for aseismic crustal deformation at Hollister, California, J. Geophys. Res. 91 (1986) 12661–12674.

[23] Mogi K., Some features of recent seismic activity in and near Japan {2}: activity before and after great earthquakes, Bull. Eq. Res. Inst. Univ. Tokyo 47 (1969) 395–417.

[24] Mogi K., Two kinds of seismic gaps, Pageoph 117 (1979) 1172–1186.

[25] Mogi K., Seismicity in western Japan and long term earthquake forecasting, in: Simpson D.W., Richards P.G. (Eds.), Earthquake Prediction: An International Review, Maurice Ewing Ser., Vol. 4, AGU, Washington, DC, 1981, pp. 43–51.

[26] Nalbant S.S., Hubert-Ferrari A., King G.C.P., Stress coupling between earthquakes in northwest Turkey and the north Aegean Sea, J. Geophys. Res. 103 (1998) 24469–24486.

[27] Newman W., Gabrielov A., Durand T., Phoenix S.L., Turcotte D., An exact renormalization model for earthquakes and material failure. Statics and dynamics, Physica D 77 (1994) 200–216.

[28] Papazachos B., Papazachos C., Accelerated preshock deformation of broad regions in the Aegean area, Pageoph 157 (2000) 1663–1681.

[29] Parsons T., Toda S., Stein R.S., Barka A., Dieterich J.H., Heightened odds of large earthquakes near Istanbul: An interaction-based probability calculation, Science 288 (2000) 661–665.

[30] Raleigh C.B., Sieh K., Sykes L.R., Anderson D.L., Forecasting Southern California Earthquakes, Science 217 (1982) 1097–1104.

[31] Rundle J.B., A physical model for earthquakes, III, J. Geophys. Res. 94 (1989) 2839–2855.

[32] Sahimi M., Arbabi S., Scaling laws for fracture of heterogeneous materials and rock, Phys. Rev. Lett. 77 (1996) 3689–3692.

[33] Saleur H., Sammis C.G., Sornette D., Discrete scale invariance, complex fractal dimensions, and log-periodic fluctuations in seismicity, J. Geophys. Res. 101 (1996) 17661–17677.

[34] Sammis C.G., Smith S., Seismic cycles and the evolution of stress correlation in cellular automaton models of finite fault networks, Pure Appl. Geophys. 155 (1999) 307–334.

[35] Sammis C.G., Sornette D., Saleur H., Complexity and earthquake forecasting, in: Rundle J.B., Klein W., Turcotte D.L. (Eds.), Reduction and Predictability of Natural Disasters, SFI Studies in the Sciences of Complexity, Vol. XXV, Addison-Wesley, Reading, MA, 1996, pp. 143–156.

[36] Savage J.C., A dislocation model of strain accumulation and release at a subduction zone, J. Geophys. Res. 88 (1983) 4948–4996.

[37] Simpson R.W., Reasenberg P.A., Earthquake-induced static stress changes on central California faults, in: Simpson R.W. (Ed.), The Loma Prieta, California Earthquake of October 17, 1989 – Tectonic process and models, US Geol. Surv. Prof. Pap., 1550-F, F55-F89, 1994.

[38] Sornette D., Sammis C.G., Complex critical exponents from renormalization group theory of earthquakes: implications for earthquake predictions, J. Phys. I 5 (1995) 607–619.

[39] Sornette A., Sornette D., Earthquake rupture as a critical point: consequences for telluric precursors, Tectonophysics 179 (1990) 327–334.

[40] Stein R.S., Barka A.A., Dieterich J.H., Progressive failure on the North Anatolian fault since 1939 by earthquake stress triggering, Geophys. J. Int. 128 (1997) 594–604.

[41] Sykes L.R., Jaumé S., Seismic activity on neighboring faults as a long-term precursor to large earthquakes in the San Francisco Bay Area, Nature 348 (1990) 595–599.

[42] Working Group on California Earthquake Probabilities, Probabilities of large earthquakes in the San Francisco Bay region, California, US Geol. Surv. Circ. 1053, 1990.

[43] Working Group on California Earthquake Probabilities, Seismic hazards in southern California: probable earthquakes, 1994–2024, Bull. Seismol. Soc. Am. 85 (1995) 379–439.